POLARIMETRIC RADAR DATA DECOMPOSITION AND INTERPRETATION

Guoqing Sun[1] and K. Jon Ranson[2]

[1] Science Systems & Application, Inc. 5900 Princess Garden Parkway, Suite 300, Lanham, MD, 20706, USA.
[2] Biospheric Sciences Branch, GSFC Greenbelt, MD 20771, USA.

1. INTRODUCTION

Significant efforts have been made to decompose polarimetric radar data into several simple scattering components. The components which are selected because of their physical significance can be used to classify SAR image data. If particular components can be related to forest parameters, inversion procedures may be developed to estimate these parameters from the scattering components.

Several methods (van Zyl, 1989; Freeman and Durden, 1992; van Zyl, 1992) have been used to decompose an averaged Stoke's matrix or covariance matrix into three components representing odd (surface), even (double-bounce) and diffuse (volume) scatterings. With these decomposition techniques, phenomena, such as canopy-ground interactions, randomness of orientation and size of scatterers, can be examined from SAR data.

In this study we applied the method recently reported by van Zyl (1992) to decompose averaged backscattering covariance matrices extracted from JPL SAR images over forest stands in Maine, USA. These stands are mostly mixed stands of coniferous and deciduous trees. Biomass data have been derived from field measurements of DBH and tree density using allometric equations. The interpretation of the decompositions and relationships with measured stand biomass are presented in this paper.

2. DECOMPOSITION

van Zyl (1992) showed that for azimuthally symmetrical terrain in the monostatic case, the average covariance matrix of backscattering can be decomposed as:

$$[T] = C \begin{bmatrix} 1 & 0 & \rho \\ 0 & \eta & 0 \\ \rho^* & 0 & \xi \end{bmatrix} = \sum_{i=1}^{3} \lambda_i k_i k_i^+ \qquad (1)$$

where $C = \langle S_{hh} S_{hh}^* \rangle$, $\rho = \langle S_{hh} S_{hv}^* \rangle$, $\eta = 2\langle S_{hv} S_{hv}^* \rangle / C$, $\xi = \langle S_{vv} S_{vv}^* \rangle / C$. The $\lambda_i, i=1,2,3$ are the eigenvalues of $[T]$. $k_i, i=1,2,3$ are the corresponding eigenvectors and + means *adjoint*. Since the eigenvectors are unitary vectors and the sum of the eigenvalues equals the total power of the backscattering, $\lambda_1, \lambda_2, \lambda_3$, are the backscattering powers contributed by odd, even and diffuse backscattering components, respectively. We also note that the λ_3 is exactly the backscattering power at cross-polarizations, i.e. $2\langle S_{hh} S_{hv}^* \rangle$. In terms of backscattered power, this algorithm decomposes the power from co-polarized returns into odd and even scattering components. For those targets with $\rho = 0$, depending on the $\xi > 1$ *or* $\xi < 1$, one of the two eigen values (either λ_1, or λ_2) equals the HH return and the other the VV return. When $\xi = 1$, the odd and even scattering components are equal.

3. RESULTS AND DISCUSSION

3.1. Decomposition and Forest Biomass

Figure 1 presents scatter plots of total above-ground fresh biomass of 47 forest stands versus $\lambda_1,\lambda_2,\lambda_3$ and σ^o at HH, HV and VV polarizations at L band. Table 1 summarizes the correlation coefficients for scattering components and measured biomass. Comparing the two plots in the third row demonstrates that λ_3 (diffuse scattering) is identical to the sum of the cross-polarization backscatter cross sections. The $\lambda 2$ (even scattering component) has higher correlation with biomass than the odd scattering component. In the first-order backscatter models, the odd scattering is from crown backscattering and direct backscattering from ground surface. If the canopy is dense and tall, crown backscattering will be the major source and the odd scattering should have higher correlation with forest biomass. This is not obvious from the data shown in Figure 1 or listed in Table 1.

3.2. Decomposition and Forest Classes

Table 2 lists the decomposition results of several classes at C, L, and P bands. Generally, the odd scattering is always the major component. The even scattering component is higher for forest stands with large and dense trees at L and P bands. The higher entropy values of dense forest stands at L and P bands show a high degree of disorder (randomness) of scatterers. At C band, except for Bog and Red Pine sites, all sites have the similar entropies.

3.3. Decomposition of modeled Scattering

Backscatter models (Sun, 1990) were used to simulate backscattering from the 47 stands. The tree density and size for a stand were from field measurements, but trees were assumed to be pure hemlocks and the ground surface to be a rough surface similar to an old cut area near these stands. The decomposition of SAR data and modeled scattering matrices at L band were compared in Figure 2. The simulated components have good correlation with biomass. Though the comparison between SAR and simulated data is crude, it seems that model gives reasonable results in terms of even and diffuse scattering but not for odd scattering.

4. SUMMARY

The decomposition method partitions the co-polarization return into odd and even scattering components. The partition depends on two parameters, i.e. ρ and ξ only. It helps to classify radar polarimetry return into general groups of scattering behavior.

The HV backscatter or diffuse components has the best correlation with forest biomass.

Comparing to HV backscatter, HH and VV backscatters have higher signal to noise ratio and are desirable for developing an inversion algorithm for forest parameter estimation. More works, however, need to be done to separate scattering components heavily influenced by ground surface from the co-polarization signatures.

REFERENCES

Freeman, A. and S. Durden, 1992, Fitting a three-component scattering model to polarimetric SAR data, *Summaries of the Third Annual JPL Airborne Geoscience Workshop*, Volume 3, AIRSAR Workshop, Ed. J. van Zyl, pp. 56-58.

Sun, G., 1990, Radar Backscatter Modeling of Coniferous Forest Canopies, Ph. D. Dissertation, University of California, Santa Barbara. 126 p.

van Zyl, J. J., 1989, Unsupervised classification of scattering behavior using radar polarimetry data, *IEEE Transactions on Geoscience and Remote Sensing, Vol. 27, No. 1*, pp. 36-45.

van Zyl, J. J., 1992, Application of Cloude's target decomposition theorem to polarimetric imaging radar data, *Proceedings of SPIE, Vol. 1748, Radar Polarimetry, Eds. H. Mott and* W. M. Boerner, 23-24 July 1992, San Diego, California, pp. 184 - 191.

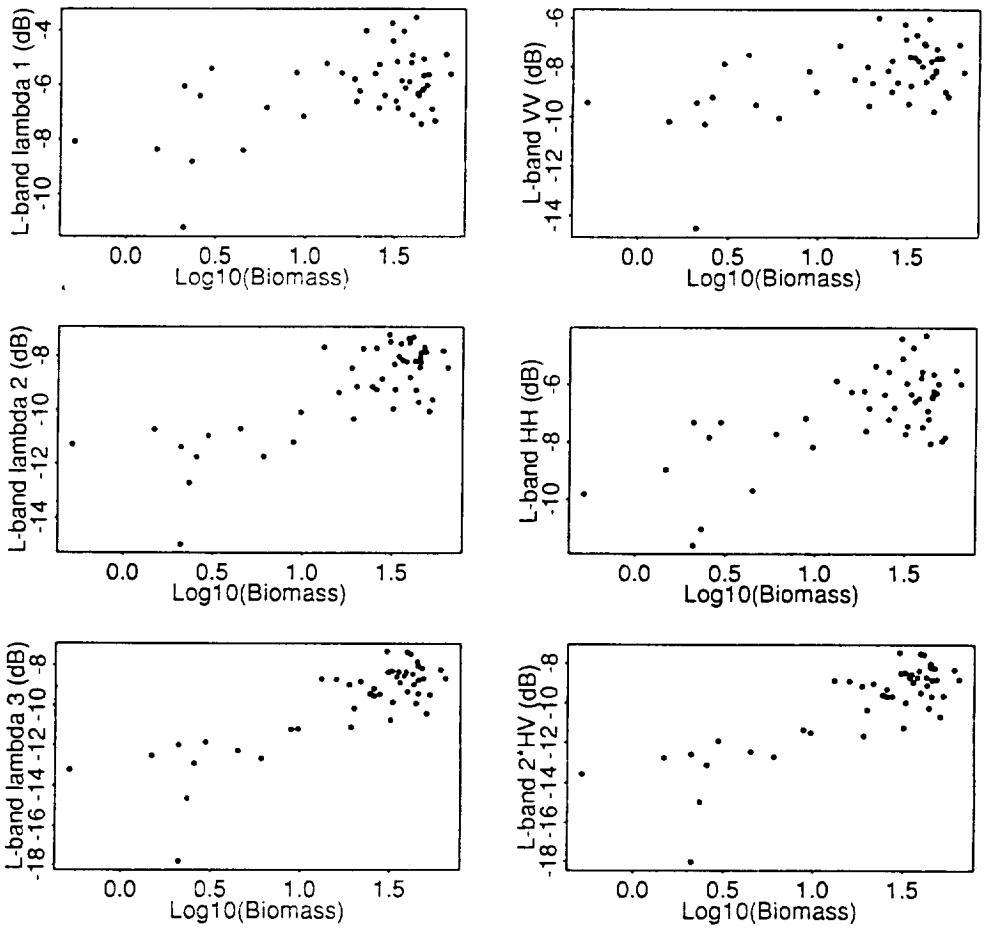

Figure 1. Comparisons of SAR original HH, VV and HV backscattering with decomposed scattering in terms of their relation to total above-ground fresh biomass.

Table 1. List of correlation parameters to biomass for variables in Figure 1 ($y = b_0 + b_1 x$).

	b_0	b_1	R^2	F-value	R.S.E
λ_1	2.470	0.193	0.281	17.54	0.436
λ_2	3.458	0.237	0.601	67.79	0.3245
λ_3	3.260	0.201	0.680	95.73	0.291
VV	2.971	0.202	0.316	20.80	0.425
HH	2.843	0.225	0.455	37.59	0.379

Table 2. Decomposition of SAR data at C, L and P bands.

Site	λ_1(%)	λ_2(%)	λ_3(%)	Total Power	Entropy
C Band					
Grass	57.94	23.09	18.97	0.2176	0.8829
Bog	78.15	12.02	9.83	0.5508	0.6147
Regen	58.71	23.16	18.13	0.3183	0.8748
Clear	61.84	20.34	17.82	0.4676	0.8451
Aspen	57.73	20.49	21.78	0.4632	0.8865
Mixed	63.55	19.74	16.71	0.4382	0.8259
Hemlock	62.64	20.73	16.63	0.4385	0.8352
Red Pine	49.38	21.59	29.03	0.2596	0.9452
Spruce	60.71	20.01	19.28	0.5368	0.8576
L Band					
Grass	81.88	10.56	7.56	0.0700	0.5429
Bog	84.00	8.03	7.97	0.3086	0.5011
Regen	53.14	25.56	21.30	0.1900	0.9230
Clear	61.32	21.48	17.20	0.3105	0.8492
Aspen	42.54	30.73	26.73	0.3921	0.9820
Mixed	46.42	29.89	23.69	0.3746	0.9634
Hemlock	45.69	28.27	26.04	0.4263	0.9698
Red Pine	44.06	27.68	28.24	0.5585	0.9774
Spruce	50.73	27.13	22.14	0.5488	0.9394
P Band					
Grass	89.64	6.87	3.49	0.0848	0.3631
Bog	88.48	6.32	5.20	0.1622	0.3975
Regen	60.42	25.01	14.57	0.1516	0.8480
Clear	63.24	22.16	14.60	0.2245	0.8230
Aspen	52.37	23.18	24.45	0.3627	0.9303
Mixed	49.13	30.07	20.80	0.3474	0.9440
Hemlock	48.83	28.37	22.80	0.4596	0.9508
Red Pine	58.95	24.64	16.41	0.6692	0.8677
Spruce	53.43	25.28	21.29	0.4608	0.9210

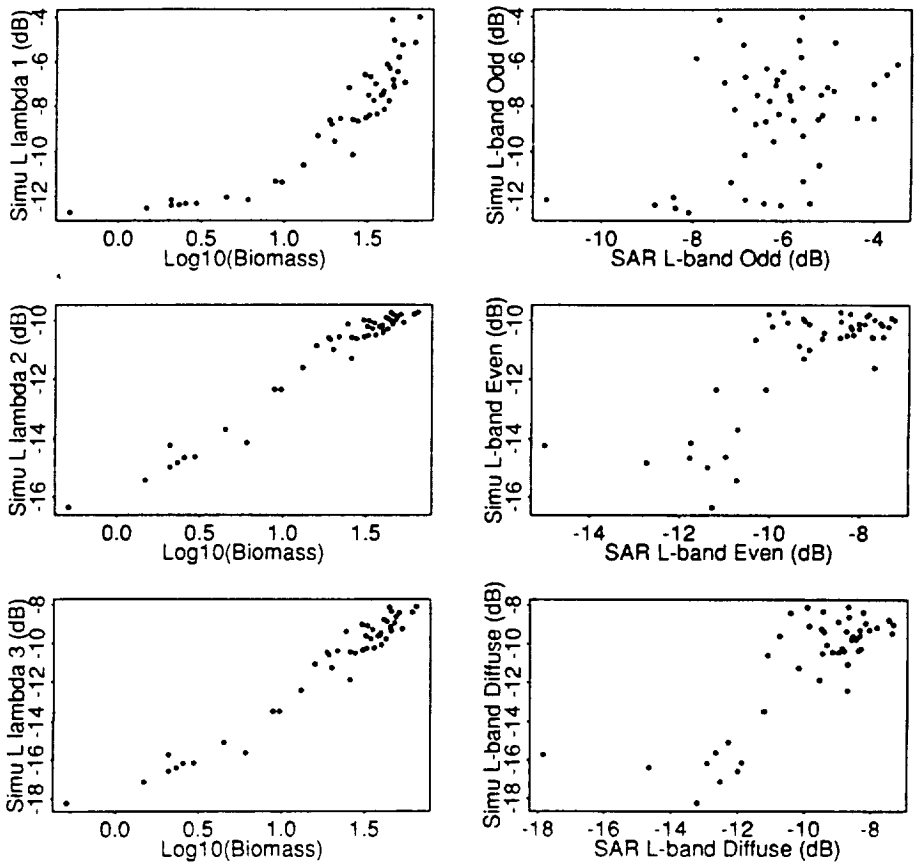

Figure 2. Decompositions of modeled backscattering and comparison with SAR data.

C-2